SOURCE PARAMETERS OF THE BORREGO MOUNTAIN EARTHQUAKE[1]

By MAX WYSS
LAMONT-DOHERTY GEOLOGICAL OBSERVATORY OF COLUMBIA UNIVERSITY
AND
THOMAS C. HANKS
SEISMOLOGICAL LABORATORY, CALIFORNIA INSTITUTE OF TECHNOLOGY

ABSTRACT

Spectral analysis of teleseismic body phases at several azimuths was used to determine the moment, fault length, dislocation, stress-drop, and radiated energy of the Borrego Mountain earthquake. The results agree well with the same parameters obtained from the surface fracture and aftershock distribution and local observations of radiated energy.

INTRODUCTION

The Borrego Mountain earthquake provided an ideal opportunity to check the reliability of teleseismic methods to estimate the moment, dimension, and dislocation of a seismic source. Although the event was large enough to be recorded by the WWSSN (Worldwide Standard Seismograph Network) at all epicentral distances, it was small enough to be recorded well on the Wood-Anderson instruments (magnification = 100) operating at Pasadena and Riverside. More important, this earthquake produced a well-defined surface rupture with a measured right-lateral displacement (Allen and others, 1968; Clark, this volume). Detailed studies of the aftershock sequence provided further information on the extent of the source region (Hamilton, this volume).

In the equivalent double-couple representation of a seismic source (Burridge and Knopoff, 1964), the seismic moment M_0 (Maruyama, 1963; Haskell, 1964) was shown by Aki (1966) to be proportional to the product of the fault area A and the average dislocation $\bar{u}$

$$M_0 = \mu A \bar{u} \qquad (1)$$

where μ is the shear modulus in the source region. With this relation, M_0 can be evaluated from field measurements of $\bar{u}$ and A, the latter calculated from rupture length and depth based on field mapping and aftershock studies. Provided that the dislocation theory models an earthquake source correctly, M_0 can be determined from the long-period amplitude spectral density (Ω_0) of body or surface waves. The two independently obtained values of M_0 will be compared in order to check the validity of the dislocation theory. Previous comparisions of teleseismically estimated M_0 with that obtained from fault area and surface displacement suffered from considerable uncertainties in the field observations (Aki, 1966; Wyss and Brune, 1968).

Another important parameter that can be estimated from teleseismic spectral data is the source dimension r. Kasahara (1957) has related the corner/peak frequency f_0 of P-wave spectra to the radius of a spherical source model. Berckhemer and Jacob (1968) have estimated the rupture area of deep earthquakes using f_0 of P-waves. Brune (1970) proposed a relation between f_0 of S-waves and the radius of a circular rupture area. The present results are a part of a larger study, one purpose of which is to check if any one of the proposed relations between f_0 and r is correct for earthquakes with known rupture length.

ACKNOWLEDGMENTS

Helpful discussions with J. N. Brune, C. B. Archambeau, and W. R. Thatcher are gratefully acknowledged. We also thank L. R. Sykes, R. V. Sharp, B. Isacks, and R. M. Hamilton for critically reading the manuscript. Some of the work was completed while the senior author was at the Institute of Geophysics and Planetary Physics, University of California, La Jolla. This research was supported by National Science Foundation grants NSF GA-19473, NSF GA-12868, and NSF GA-22709.

[1]Contribution 1819, Lamont-Doherty Geological Observatory and Contribution 1930, Division of Geological Sciences, California Institute of Technology, Pasadena, Calif.

DATA

The vertical components of P-waves recorded at eight WWSSN locations (table 4) at distances between 37° and 86° were Fourier-analyzed; the resulting displacement spectra $\Omega(\omega)$ and their azimuthal distribution are shown in figure 10. In order to cover as large a frequency range as possible, the spectra of the long-period records as well as of the short-period records have been determined and plotted on the same graph. $\Omega(\omega)$, as presented in figures 10 and 11, has been corrected for the instrument response and for attenuation using the results of Julian and Anderson (1968) for an earth model MM8 (Anderson, Ben-Menahem, and Archambeau, 1965). The units of $\Omega(\omega)$ are given in centimeter-seconds for both P- and S-waves.

The S-wave spectra of four stations are shown in figure 11. Only one station furnished a usable short-period record. The corner frequency f_0, however, is clearly defined by the long-period spectra alone. In order to avoid contamination of the S phase by other phases, only stations between 63° and 75° were considered. The window length ranged from 30 to 60 seconds.

P- and S-wave spectra were also recorded at local stations (Pasadena, Δ=220 km; and Riverside, Δ=145 km). The recordings were obtained from low-magnification Wood-Anderson instruments (gain=100). These data were considered useful only in the range $0.5 \leq f \leq 2.5$ Hz. Although these data will not be useful in the moment or source dimension determinations, they provide a lower bound check for the radiated seismic energy.

In order to estimate the moment and the total radiated energy, the following corrections of the spectral amplitudes measured at any station have been made. For the combined displacement amplification by the free surface and the crust at the receiver, an average value of 2.5 for P and S has been assumed (Ben-Menahem and others, 1965). For the radiation pattern correction, a vertical right-lateral strike-slip source with strike azimuth of N. 48° W. was used. The decrease in amplitude due to geometrical spreading was accounted for, and the spatial integration of the energy radiated in different directions was performed using Wu's (1966) results. Because of the presence of the free surface at the source, only half of the integral given by Wu (1966) for the whole space was taken for the energy integration.

SEISMIC MOMENT

At the long-period end, $50 \geq T \geq 10$ sec, the spectral amplitudes are approximately constant and at shorter periods fall off approximately as ω^{-2}, where $\omega = \frac{2\pi}{T}$. The long-period levels have been approximated as indicated in figures 10 and 11 and given as Ω_0 in table 4. This approximation of the spectrum is in accordance with the results of dislocation theory (Aki, 1967; Brune, 1970), provided that the spectral information in this period range is a meaningful representation of the ultralong-period level. On the other hand, the lack of data for $T > 50$ sec admits the possibility that the chosen level may only be the maximum of a broad peak as required by Archambeau (1968). The seismic moment M_0 was estimated from the corrected Ω_0 using equations for the far-field dynamic displacement by Keilis-Borok (1960) and Ben-Menahem, Smith, and Teng (1965).

The moments obtained from teleseismic spectra are in good agreement with the moments estimated from field observations. M_0 obtained from the different stations are given in table 4.

TABLE 4. — *P- and S-wave spectral data*

Station code	Dist. Δ (deg)	Az from epicenter (deg)	Az from station (deg)	Phase	Component	Long-period amplitude Ω_0 (cm-sec)	Corner frequency f_0 (Hz)	Dimension $r=L/2$ (km)	Moment M_0 (10^{25} dyne-cm)	Energy E (10^{19} erg)
AKU	63.4	27	292	S	EW	$2.2 \cdot 10^{-2}$	0.069	17.4	5.9	3.8
AKU				S	NS	$1.4 \cdot 10^{-2}$	.05	24.0	5.9	3.8
ESK	74.9	33	307	P	Z	$5.0 \cdot 10^{-4}$	.20	10.5	—	—
ESK				S	EW	$1.6 \cdot 10^{-2}$	.063	19.0	8.1	8.0
ESK				S	NS	$2.5 \cdot 10^{-2}$	.063	19.0	8.1	8.0
NAT	85.4	99	304	P	Z	$1.4 \cdot 10^{-3}$	.22	9.5	[11.]	—
TRN	54.8	101	303	P	Z	$3.5 \cdot 10^{-3}$	.126	16.7	11.	1.6
LPB	67.4	129	318	P	Z	$3.3 \cdot 10^{-3}$	.12	17.5	—	—
LPB				S	EW	$1.4 \cdot 10^{-2}$	.052	23.1	7.0	3.3
LPB				S	NS	$2.0 \cdot 10^{-2}$	.05	24.0	7.0	3.3
ARE	65.2	132	320	P	Z	$3.2 \cdot 10^{-3}$	.16	13.1	—	—
ARE				S	EW	$1.6 \cdot 10^{-2}$	.063	19.0	5.5	2.5
ARE				S	NS	$2.0 \cdot 10^{-2}$	.047	25.5	5.5	2.5
KIP	38.8	263	63	P	Z	$4.0 \cdot 10^{-3}$	.16	13.0	7.4	1.5
MAT	81.9	308	55	P	Z	$1.8 \cdot 10^{-3}$	.21	10.0	—	—
COL	37.1	338	133	P	Z	$5.0 \cdot 10^{-3}$	.126	16.7	12.0	1.9

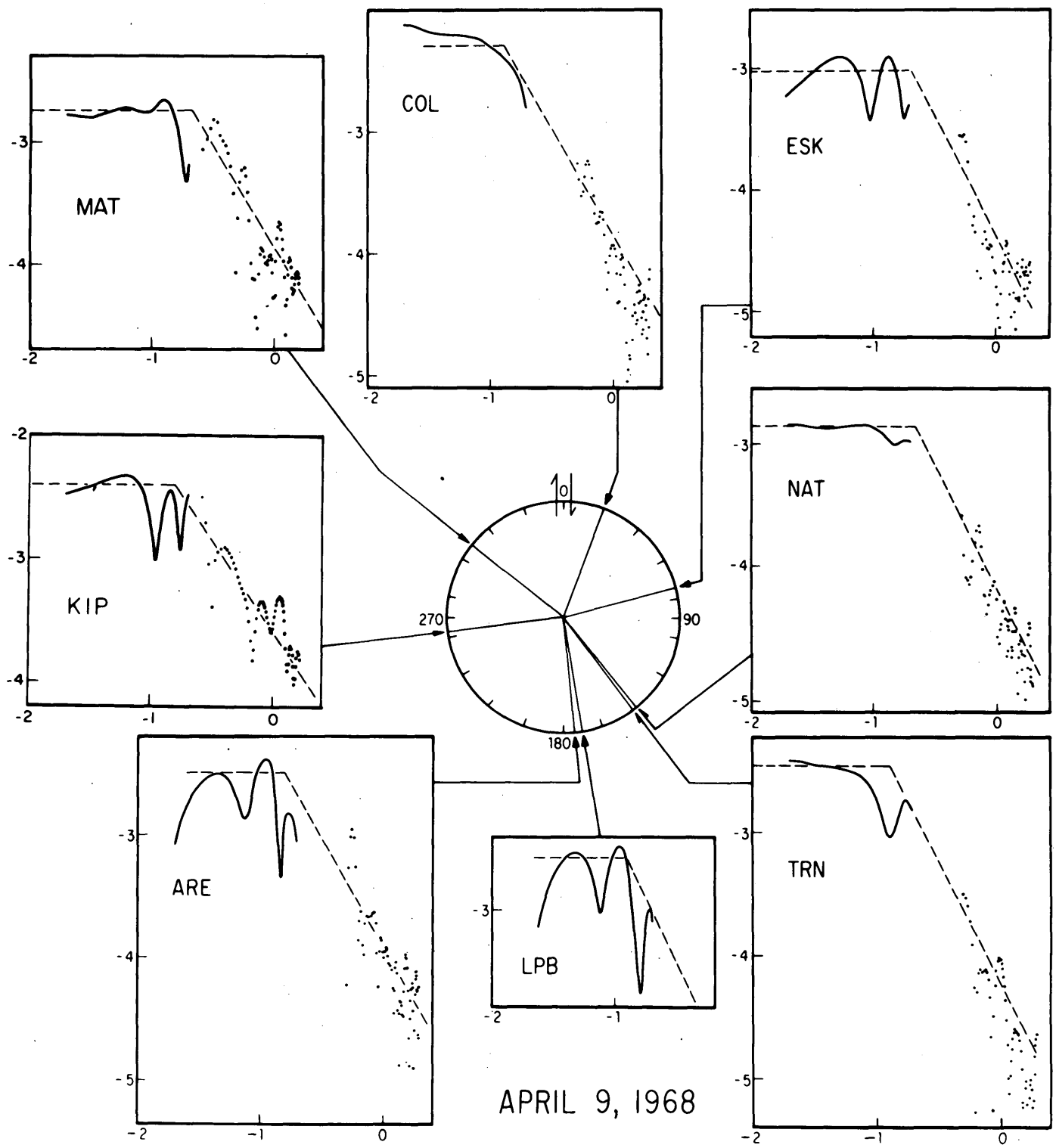

FIGURE 10. — Attenuation-corrected P-wave spectra of the Borrego Mountain earthquake. Solid line obtained from long-period vertical WWSSN instruments, and dots obtained from short-period vertical WWSSN instruments. Azimuths with respect to strike of fault. Vertical scale is log of displacement spectra, in centimeter-seconds; horizontal scale is log frequency, in Hertz.

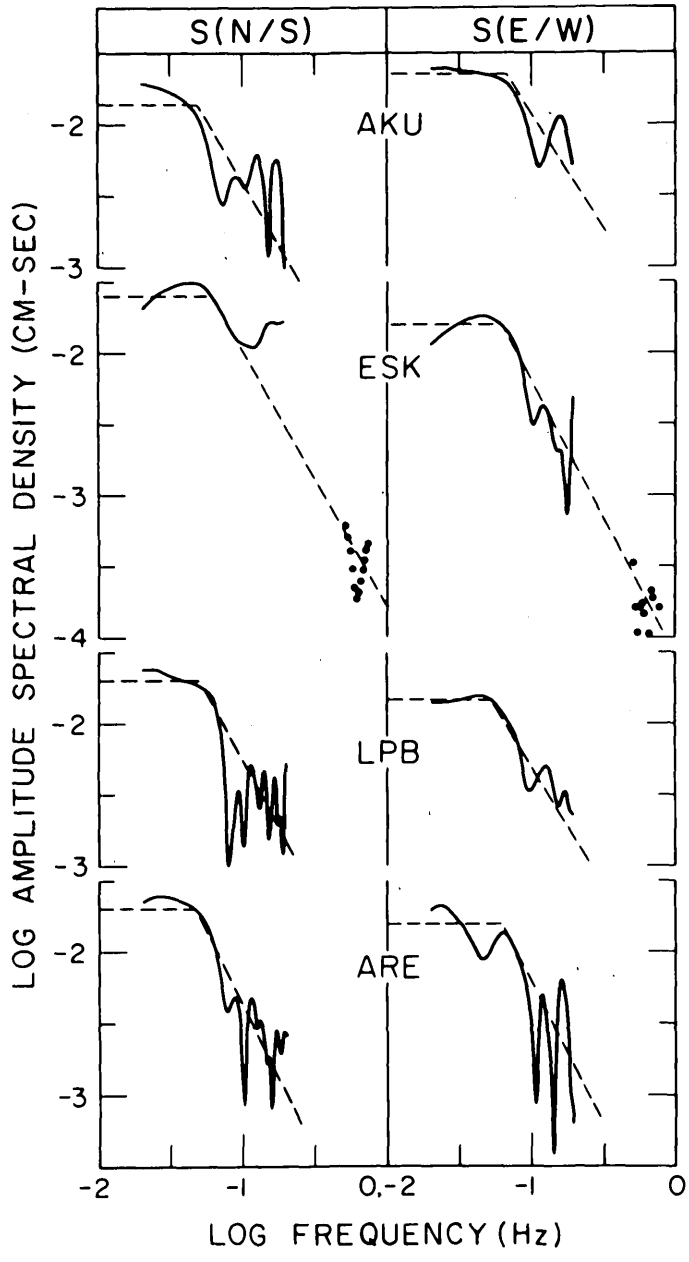

FIGURE 11. — Attenuation-corrected S-wave spectra of the Borrego Mountain earthquake from WWSSN recordings.

Unfortunately, some stations were close to nodes in the P-wave radiation pattern. If the correction due to the radiation pattern alone was larger than a factor of 10, the moment was not computed, since small uncertainties in the focal mechanism could introduce large errors. The average of the P- and S-wave moments of table 4 is compared with M_0 derived from observations in the source area in table 5. The depth of faulting was assumed to be the depth to which the aftershock activity extended, $h=12$ km (Hamilton, this volume). M_0, based on teleseismic (dynamic) measurements, agrees within approximately a factor of 2 with the field (static) observations.

The teleseismically determined moments are likely to be affected by reflections from the free surface. The inclusion of pP in the spectral analysis is expected to cause an overestimate of M_0. This may explain why the teleseismic moments are larger than the static ones (table 5). The long-period data, however, do not indicate the expected degradation of the radiation at periods long compared to the timelag Δt of the reflected phase ($\Delta t \simeq \frac{2h}{\alpha} \leq 3$ sec; h=source depth $\leq$ 10 km, α=P-wave velocity=6.0 km/sec). The facts that the Borrego Mountain earthquake ruptured the surface and had a depth of rupture comparable to the length of rupture undoubtedly complicates an image point source representation of reflected phases. Other error sources for individual stations are uncertainties in the fault plane solution and the effect of local upper mantle and crustal structure. These two effects could combine to form an error that in general should not exceed a factor of three in the moment determination for any one station. In the average moment determination from the several stations, some of these errors should be cancelled out, and it is encouraging to see that the RMS (root mean square) errors are small (table 5).

TABLE 5.—*Source parameters*

Field observation or spectral estimate	Moment M_0 (10^{25} dyne-cm)	Length $L=2r$ (km)	Area A_0 (km^2)	Depth h (km)	Dislocation $\bar{u}$ (cm)	Stress-drop $\Delta\sigma$ (bar)
Surface rupture	3.6	33	396	[1]12	30	4
Aftershock zone	4.9(6.1)	45(56)	540(672)	12	30	–
P-wave (Brune)	10.±2	26±6.5	615	–	30	20
S-wave (Brune)	6.6±1	42±6	1460	–	14	3
P-wave (Kasahara)	–	8	53	–	–	–
P-wave (Berckhemer and Jacob)	–	8.5	58	–	–	–

[1]Assumed from aftershock distribution.

The moments obtained from field observations will be affected by errors in the estimates of the rupture area and the dislocation. The zone of intense aftershock activity in the figures shown by Hamilton (this volume) is 45 km long. If the sporadic aftershock activity toward the north is included, a length of 56 km is obtained. We feel, however, that the intense aftershock zone outlines the rupture area, whereas the more northern events were caused by strain accumulations beyond the fault end. This view is supported by the Coyote Mountain earthquake of April 28, 1969, and

its aftershock sequence, which were located in this zone of sporadic aftershock activity, 33°20'N., 116°21'W. (R. M. Hamilton, oral commun., 1970; Thatcher and Hamilton, 1971). Even though we feel that 45 km is the value that should be used for the fault length as outlined by the aftershocks, the source parameters based on 56 km are also computed and given in table 5 in parentheses. The length of the surface rupture differs by a factor of 1.3 (1.7) from the extent of the intense (extended) aftershock activity. The depth of the main shock given by Allen and Nordquist (this volume) is 11 km, which differs from the depth of the deepest aftershocks by a factor of 1.1. These factors may combine to an error of less than 2 in the area estimates. Insofar as no creep occurred on the northern branch of the fault, three-quarters (Brune and Allen, 1967) of the maximum surface displacement, 38 cm (Clark, "Surface Rupture Along the Coyote Creek Fault," this volume), was taken to represent the average displacement at depth. It is hard to imagine that the displacement could be in error by more than a factor of 3. Under this assumption, the statically estimated moment might be uncertain to a factor of 5. This is an extreme value, however, and we believe that the static moment is estimated to within a factor of 3 from the correct value.

The agreement in table 5 can be considered very good, and it is concluded that the moment of a double-couple source can be determined equally well from teleseismic body phases or from field observations in the source region.

FAULT LENGTH

The corner frequency f_0 was defined by the intersection of the horizontal line representing the long-period spectral level and the line drawn through the short-period data, if they were available. Otherwise, f_0 was estimated from the decay of the long-period data.

Brune (1970) related f_0 for S-waves to the source dimension r by

$$r=\frac{2.21\beta}{2\pi f_0(\mathrm{S})}=\frac{1.2}{f_0(\mathrm{S})}, \tag{2}$$

where r is measured in kilometers.

Because the flat amplitude level at frequencies smaller than f_0 is due to interference of waves with wavelength λ longer than the source size, it would seem reasonable to obtain a version of equation 2 valid for P-waves by keeping λ_0 constant and substituting α, the P-wave velocity, for β, the S-wave velocity. To estimate the source dimension from the P-wave spectra, we use the relation

$$r=\frac{2.21\alpha}{2\pi f_0(\mathrm{P})}=\frac{2.1}{f_0(\mathrm{P})}. \tag{3}$$

The source radii obtained from 2 and 3 and the appropriate f_0 are given in table 4. The values from stations at different azimuths are generally consistent, indicating that such effects as focusing due to rupture propagation, substation crustal reverberations, and 6-second microseisms are not sufficient to disguise the gross behavior of body-wave spectra of the Borrego Mountain earthquake.

Averages for the P- and S-wave determinations of $L=2r$ and of the ruptured area $A=\pi r^2$ are compared to surface rupture and aftershock length in table 5. The agreement between the four length determinations is very close, if Brune's equations are used, and it is concluded that the source dimensions of an earthquake can be obtained with satisfactory accuracy from spectral P- and S-wave analysis using Brune's (1970) results. It is to be noted, however, that the source dimensions obtained from P-wave spectra are consistently smaller than those from S-wave spectra. This fact may indicate that the step from equation 2 to equation 3 is not completely correct and needs clarification.

Kasahara's (1957) model relates the radius of a spherical source to f_0 by

$$r=\frac{0.66}{f_0(\mathrm{P})}. \tag{4}$$

If the average value for f_0 (P) from table 4 is used in equation 4, we obtain $L=2r=8.2$ km. In Berckhemer and Jacob's (1968) theory, the maximum rupture velocity c has to be assumed; their relation is

$$A_0=\frac{c^2}{f_0^2}\frac{1}{2\pi}. \tag{5}$$

Even if a rather high rupture velocity of 3 km/sec is assumed, the average area A_0 from 5 is only 58 km^2. The diameter of a circular fault with this area is approximately 8.5 km.

The values for A_0 and r that are estimated by equations 3, 4, and 5 are compared in table 5 to the values observed in the source region. It is evident that the theories of earlier authors (Kasahara, Berckhemer, and Jacob) underestimate the source dimensions, but Brune's relation gives results which are in excellent agreement with the field observations.

The use of body waves for source size determination has great advantages over the surface wave method (Ben-Menahem, 1961). The excitation of surface waves is strongly dependent on the crustal structure, and the source depth interference can be severe (Tsai, 1969). Also, for smaller events it is

difficult to extend surface wave spectra to the short periods required without mode contamination, and deep earthquakes often do not excite measurable surface waves. A disadvantage of the body-wave method is that at a range of shallow depths the surface reflections pP and sS cannot be separated from the direct phase, and the interference of these phases with the direct waves can be expected to complicate the analysis.

ENERGY ESTIMATES

The energy in a body wave spectrum is proportional to $\int_{-\infty}^{\infty} |\Omega(\omega)\omega|^2 d\omega$. For a theoretical spectrum as given by Haskell (1964), Aki (1967), or Brune (1970), the energy integral can be conveniently represented by $\Omega_0^2 f_0^3$

$$E_s = k\Omega_0^2 f_0^3. \quad (6)$$

The constant k contains corrections for geometrical spreading, free surface and crustal effects at the station, the radiation pattern, integration of the radiation pattern over the focal sphere, rate of decay of the spectrum for $\omega > \omega_0$ (here assumed to be ω^{-2}), as well as material constants. The energy radiated from a surface source into the halfspace below was taken to be half the integral given by Wu (1966) for a whole space. The total energy radiated by the Borrego Mountain earthquake as P- and SH-waves is given in table 4; the average teleseismic estimates are $E(\mathrm{SH}) = 0.44 \cdot 10^{20}$ ergs, $E(\mathrm{P}) = 0.16 \cdot 10^{20}$ ergs. The teleseismic observations indicate that the total radiated energy, including SV, was approximately $0.69 \cdot 10^{20}$ ergs.

The radiated seismic energy has also been estimated from the seismograms written by the Wood-Anderson torsion seismograph operating at a gain of 100 at Pasadena and Riverside. Table 6 gives estimates of the seismic energy radiated for all components of P- and SH-waves in the frequency range $0.5 \leq f \leq 2.5$ Hz. The bulk of the seismic energy, however, is not included in the above estimate, because the corner frequency occurs outside of the frequency range available for analysis. We can check whether the locally recorded spectra agree approximately with the teleseismic ones by extrapolating the slope of the local spectra as a straight line to lower frequencies. At the average corner frequency, this straight line should intersect with the long-period flat level of the spectrum, which at that particular station corresponds to the average moment. The agreement is fairly good. If we assume that the long-period level corresponding to the average moment, the corner frequency, and the slope of spectral decay to high frequencies are given, we estimate the total radiated energy based on the Pasadena record to be approximately $2 \cdot 10^{20}$ ergs.

TABLE 6.—*Local observations of radiated seismic energies*

Station and Phase	Energy, 10^{19} ergs[1]
Pasadena:	
P(Z)	1.3
S(NS)	2.3
S(EW)	2.5
Riverside:	
P(Z)	2.6
S(NS)	.9
S(EW)	1.0

[1]Estimate based on spectral amplitudes corrected for seismic attenuation, with $Q=500$ in the bandwidth $0.5 \leq f \leq 2.5$ Hz.

The energy estimated from the energy-magnitude relationship (Gutenberg and Richter, 1956) amounts to several times 10^{21} ergs, depending on the relation used. The spectral estimates discussed above are an order of magnitude smaller. The energies estimated by integration agree with the energy estimated by DeNoyer (1959) for earthquakes with comparable magnitude. The problem of energy should be studied in detail, but for this task complete spectra, including the corner frequency from nearby stations, are needed.

An interesting result is that the ratio of the S-wave to the P-wave energy is 3.3 despite the considerably larger long-period S-wave amplitudes. Since the energy is a function of the ratio of amplitude over period, the larger long-period S-wave amplitudes are partly offset by a smaller f_0 (S). This relation is best understood in terms of equation 6, where Ω_0 is proportional to $\frac{1}{v^3}$, while f_0 and k are proportional to v (v=respective propagation velocity). Therefore, the ratio of S to P wave energy should be $(\alpha/\beta)^2 \simeq 3$. Gutenberg and Richter (1956) assumed a ratio of 2; this ratio agrees with our observation.

STRESS-DROP

The stress-drop $\Delta\sigma = \sigma_1 - \sigma_2$ (σ_1=stress prior to rupture, σ_2=stress after completion of the event) can be estimated from the moment and the source radius through the relation (Brune, 1970)

$$\Delta\sigma = \frac{7}{16}\frac{M_0}{r^3}. \quad (8)$$

From the field observations, the stress-drop was also estimated using Knopoff's (1958) equation $\Delta\sigma = \frac{u\mu}{2h}$, where u=dislocation and h=depth. The three different estimates are given in table 5. They agree well, and the average stress-drop is $\Delta\sigma = 9$ bar. This value is much smaller than the stresses that the earth's crust is able to maintain.

From the stress-drops of large shallow earthquakes, Chinnery (1964) estimated that the crust can accumulate 100 bar shear stresses. Brune, Henyey, and Roy (1969) obtained an upper bound of 200 bars for the stresses accumulated on the San Andreas fault, based on heat-flow measurements. Evidently, the Borrego Mountain earthquake is another low stress-drop event like the Parkfield (Aki, 1967; Wyss and Brune, 1968) and the Imperial (Brune and Allen, 1967) earthquakes. This result lends further support to the observation that the stress-drop of small earthquakes is in general smaller than that of large earthquakes (King and Knopoff, 1968; Wyss, 1970).

CONCLUSIONS

With the assumption of a double-couple source model, the use of teleseismically observed body-wave spectra has been successful in determining the fault dimension and seismic moment (and, equivalently, total offset and stress-drop) of the Borrego Mountain earthquake. The results are in close agreement with independently obtained values resulting from local field observations. The average fault length is 37 km, the average moment is $6.3 \cdot 10^{25}$ dyne cm, and the average stress-drop is 9 bars.

The radiated seismic energy estimated from teleseismic observations is $0.69 \cdot 10^{20}$ erg and from local observations, extrapolated to include the whole frequency range, is $2 \cdot 10^{20}$ erg.

REFERENCES CITED

Aki, K., 1966, Generation and propagation of G waves from the Niigata earthquake of June 16, 1964. Part 2. Estimation of earthquake moment, released energy, and stress drop from the G wave spectrum: Tokyo Univ. Earthquake Research Inst. Bull., v. 44, p. 73–88.

———1967, Scaling law of seismic spectrum: Jour. Geophys. Research, v. 72, p. 1217–1231.

Allen, C. R., Grantz, A., Brune, J. N., Clark, M. M., Sharp, R. V., Theodore, T. G., Wolfe, E. W., and Wyss, M., 1968, The Borrego Mountain, California, earthquake of 9 April 1968: A preliminary report: Seismol. Soc. America Bull., v. 58, p. 1183–1186.

Anderson, D. L., Ben-Menahem, A., and Archambeau, C. B., 1965, Attenuation of seismic energy in the upper mantle: Jour. Geophys. Research, v. 70, p. 1441–1448.

Archambeau, C. B., 1968, General theory of elastodynamic source fields: Rev. Geophyics, v. 6, p. 241–287.

Ben-Menahem, A., 1961, Radiation of seismic surface waves from finite moving sources: Seismol. Soc. America Bull., v. 51, p. 401–435.

Ben-Menahem, A., Smith, S. W., and Teng, T. L., 1965, A procedure for source studies from spectrums of long-period seismic waves: Seismol. Soc. America Bull., v. 55. p. 203–235.

Berckhemer, H., and Jacob, K. H., 1968, Investigation of the dynamical process in earthquake foci by analyzing the pulse shape of body waves: Final Sci. Rept. Contract AF61(052)–801, Institute of Meteorology and Geophysics, University of Frankfurt, Germany, 85 p.

Brune, J. N., 1970, Tectonic stress and the spectra of seismic shear waves: Jour. Geophys. Research, v. 75, p. 4997–5009.

Brune, J. N., and Allen, C. R., 1967, A low stress-drop, low magnitude earthquake with surface faulting—The Imperial, California, earthquake of March 4, 1966: Seismol. Soc. America Bull., v. 57, p. 501–514.

Brune, J. N., Henyey, T. L., and Roy, R. F., 1969, Heat flow, stress, and rate of slip along the San Andreas fault, California: Jour. Geophys. Research, v. 74, p. 3821–3827.

Burridge, R., and Knopoff, L., 1964, Body force equivalents for seismic dislocations: Seismol. Soc. America Bull., v. 54, p. 1875–1888.

Chinnery, M. A., 1964, The strength of the earth's crust under horizontal shear stress: Jour. Geophys. Research, v. 69, p. 2085–2089.

DeNoyer, J., 1959, Determination of the energy in body and surface waves (Part II): Seismol. Soc. America Bull., v. 49, p. 1–10.

Gutenberg, Beno, and Richter, C. F., 1956, Earthquake magnitude, intensity, energy, and acceleration: Seismol. Soc. America Bull., v. 46, p. 105–145.

Haskell, N. A., 1964, Total energy and energy spectral density of elastic wave radiation from propagating faults: Seismol. Soc. America Bull., v. 54, p. 1811–1841.

Julian, B. R., and Anderson, D. L., 1968, Travel times, apparent velocities, and amplitudes of body waves: Seismol. Soc. America Bull., v. 58, p. 339–366.

Kasahara, K., 1957, The nature of seismic origins as inferred from seismological and geodetic observations: Tokyo Univ. Earthquake Research Inst. Bull., v. 35, p. 473–530.

Keilis-Borok, V. I., 1960, Investigation of the mechanism of earthquakes: Akad. Nauk. SSSR Geofiziki Inst. Trudy, no. 4 (166), Soviet Research in Geophysics, v. 4, (trans. by American Geophysical Union, Consultants Bureau Enterprises, New York).

King, C. Y., and Knopoff, L., 1968, Stress drop in earthquakes: Seismol. Soc. America Bull., v. 58, p. 249–257.

Knopoff, Leon, 1958, Energy release in earthquakes: Geophys. Jour., v. 1, p. 44–52.

Maruyama, T., 1963, On the force equivalent of dynamic elastic dislocations with reference to the earthquake mechanism: Tokyo Univ. Earthquake Research Inst. Bull., v. 41, p. 467–486.

Thatcher, W. R., and Hamilton, R. M., 1971, Spatial distribution and source parameters of the Coyote Mountain aftershock sequence, San Jacinto fault zone [abs.], *in* Geol. Soc. America Abs. with Programs, v. 3, no. 2, 229 p.

Tsai, Y. B., 1969, Determination of focal depths of earthquakes in the mid-oceanic ridges from amplitude spectra of surface waves: Massachusetts Inst. Technology Ph. D. thesis.

Wu, F. T., 1966, Lower limit of the total energy of earthquakes and partitioning of energy among seismic waves: California Inst. Technology, Pasadena, Ph. D. thesis.

Wyss, M., 1970, Observation and interpretation of tectonic strain release mechanisms: California Inst. Technology, Pasadena, Ph. D. thesis.

Wyss, M., and Brune, J. N., 1968, Seismic moment, stress, and source dimensions for earthquakes in the California-Nevada region: Jour. Geophys. Research, v. 73, p. 4681-4694

The Borrego Mountain Earthquake of April 9, 1968

GEOLOGICAL SURVEY PROFESSIONAL PAPER 787

Contributions from:
California Institute of Technology
Lamont-Doherty Geological Observatory of Columbia University
Seismological Field Survey, National Oceanic and Atmospheric Administration

UNITED STATES GOVERNMENT PRINTING OFFICE, WASHINGTON : 1972